Contrasts Between the Earthquakes 2005 Kashmir and 2006 South Java and Development Towards the Seismic Hazard Mapping of Java

Paul W. Burton
Seismic Risk Group, School of Environmental Sciences, University of East Anglia, Norwich, NR4 7TJ, United Kingdom, email: p.burton@uea.ac.uk
Stephen W. Cole
Seismic Risk Group, School of Environmental Sciences, University of East Anglia, Norwich, NR4 7TJ, United Kingdom, email: s.cole@uea.ac.uk

ABSTRACT

The Muzafarrabad, Kashmir 2005, 8 October, earthquake had moment magnitude 7.6 M_W and resulted in the destruction of many buildings and in a high number of fatalities. In retrospect, the Yogyakarta or Bantul earthquake of 2006, 27 May, resulted in much less loss of life but was a much smaller earthquake with a magnitude of 6.3 M_W. The Kashmir earthquake had a thrust mechanism. Direct impact of this Kashmir earthquake caused by ground movements included destruction of rural civil buildings and other similarly built structures (these are Category A and B buildings on MSK/EMS intensity scales experiencing maximum intensity I_0 X MSK) and upwards of 80,000 deaths. There were many landslides induced as a secondary hazard phenomenon but liquefaction was not a contributing phenomenon. This earthquake has a mortality rate placing it in the worst 24 worldwide during the last millennium. The Yogyakarta, Java earthquake epicenter and dynamics of the causative faulting system are unclear. Nevertheless several thousand fatalities and several hundreds of thousands of seriously damaged properties (experiencing I_0 ~IX MSK) have been reported. These are great losses. Careful analysis of seismicity and seismic hazard is important to both areas.

Hazard expectations for Java are prepared and mapped in this study. Methods used for seismic hazard analysis range from magnitude and strong ground shaking expectation examined using extreme value distributions through to cumulative strain energy release (CSER) analyses. The extreme value approach examines both magnitude recurrence and strong ground shaking expectations – hence preliminary seismic hazard maps for comparison to those already available. CSER diagrams picture changing expectations of a similar magnitude earthquake in this area and provide an indication of maximum credible expectations locally. In the case of South Java, localized near Yogyakarta, the CSER results suggest this zone may be entering a period of strain accumulation rather than release, but this does not provide reason for complacency as 50-year (with a one-in-ten chance of exceedance) expectations of peak ground acceleration reach ~300 cm s^{-2}.

Such preliminary new assessments of seismic hazard in both the Kashmir and the South Java areas, before and after these earthquakes, will allow examination of changing expectations and emphasize the need for fuller, comprehensive seismic hazard analysis. Impacts on buildings in the meizoseismal area of the Kashmir earthquake are included via field photographic evidence (from an Earthquake Engineering Field Investigation Team's visit to the area) to provide evidence of building failure mode in relation to horizontal ground displacements caused by the earthquake – these bear comparison to the Bantul earthquake and detailed studies of failure mode should also be made to assist mitigation recommendations for the future.

INTRODUCTION

The 2005 Kashmir and the 2006 Bantul earthquakes differ considerably in some respects. The Kashmir earthquake had a thrust, mountain building mechanism of major size at magnitude 7.6 M_W. The Bantul earthquake was more moderate at magnitude 6.3 M_W and had a strike-slip mechanism. However, these two earthquakes are worthy of comparison in view of their societal impact. Both occurred near urbanised areas and caused great loss to built structures and inhabitants. In both cases buildings were vulnerable, hazard and risk mapping were inadequate, and preparedness levels were low. Our aims in this paper are firstly to prepare a seismic hazard analysis for South Java following the Bantul earthquake. Secondly, the intention is to consider briefly the failure and collapse mode of vulnerable buildings during the Kashmir earthquake that were in response to the step or pulse of horizontal ground displacement generated by the faulting mechanism, and draw comparisons with the Bantul earthquake. An in-depth study of seismic hazard, vulnerability, risk assessment and related recommendations for population welfare would necessarily require a full and time consuming study in situ beyond what can be done briefly here.

EARTHQUAKE CATALOGUE AND SEISMICITY

The scientific analysis objectives of this study require an earthquake catalogue detailing standard earthquake source parameters (year-month-date/epicentre latitude-longitude/focal depth/magnitude). Data used herein are extracted from the NEIC database. The total set extracted spans all Java and the seas north and south of the mainland, viz: 3°-13°S, 105°-115°E. These data only begin in 1973 and have been chosen to extend through 2006 May 27, thus eliminating most aftershocks of the Bantul earthquake. There are 1,993 earthquakes in this earthquake catalogue. The immediate difficulty is that NEIC data are reported on various magnitude scales and for seismic hazard analysis purposes these have to be rendered homogeneously onto one magnitude scale. The surface wave magnitude scale is the target homogeneous scale as most strong ground shaking laws for attenuation of peak ground acceleration are expressed in terms of M_S. Most magnitude entries in the NEIC catalogue are on the body wave magnitude scale m_b and these are converted to M_S using the global correlation of Rezapour & Pearce (1998). A few other magnitude scale conversions were required for a much smaller number of earthquakes, the most significant being conversion from moment magnitude M_W, for which $M_W = M_S$ was adopted. The resulting study catalogue is illustrated in Figure 1.

MAGNITUDE HAZARD

Two approaches are adopted here for the assessment of magnitude hazard. The first relies on a model of seismicity and is

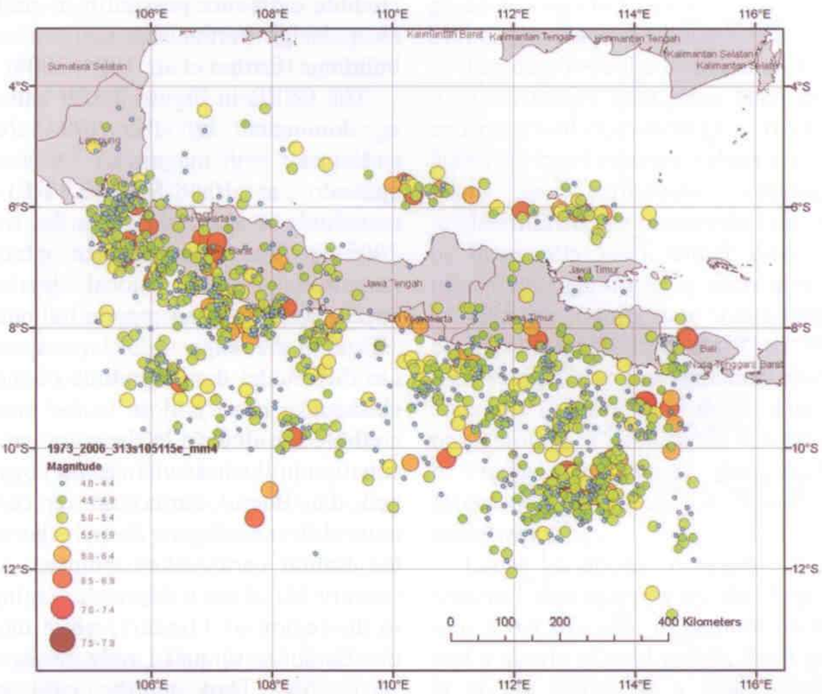

Figure 1. Seismicity in Java 1973-2006/05/27 (NEIC data homogenised to surface wave magnitude scale).

non-probabilistic in its nature: this is the Cumulative Strain Energy Release (CSER) approach. The second approach is entirely probabilistic in its nature and determines the probability of occurrence of different earthquake magnitudes. These separate approaches in juxtaposition allow useful comparisons to be made.

Cumulative Strain Energy Release (CSER)

A graphical approach to CSER and seismic moment release rates has often been used to characterise seismicity in a region. CSER diagrams can provide estimates of a magnitude equivalent to the annual average energy release M2, more importantly the magnitude equivalent to the maximum credible earthquake M3 when all energy in an earthquake cycle is released in one earthquake, and an indication of the waiting time TW between M3 events (see Makropoulos and Burton, 1984). CSER diagrams for the entire study catalogue (effectively all Java), the near-vicinity zone of the Bantul 2006 epicentre prior to the earthquake (up to end 2005) and for near-vicinity of the Bantul 2006 epicentre through 2006 May 26 are presented in Figure 2. To produce these graphs it is necessary to convert the magnitude M of an earthquake to energy release, E ergs, and there are several equations that do this. This is a fair way of looking at maximum credible (maxcred) hazard potential, compared to conventional seismic hazard assessment, and generates an earthquake magnitude that can be input to a Geographic Information System earthquake scenario to illustrate worst-conceivable consequences of an earthquake in a region for learning and mitigation purposes. It should be borne in mind, however, that a region may generate more mid-magnitude 6 earthquakes that are devastating than say a single maximum credible magnitude 7

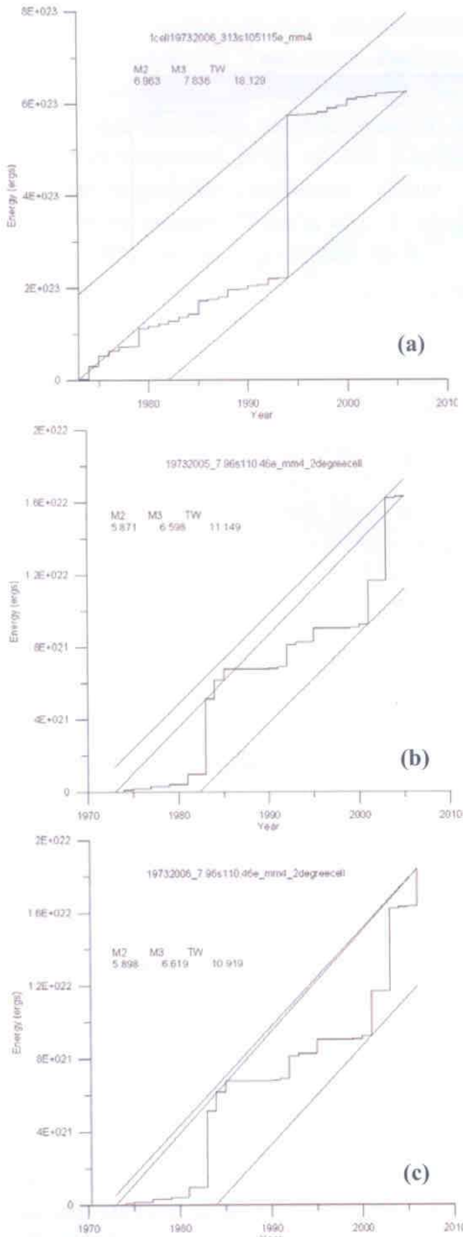

Figure 2. Cumulative strain energy release analyses for: a) 3°-13°S, 105°-115°E, b) 2° cell centred on Bantul epicentre but excluding it and c) including it.

earthquake while the release of strain energy or seismic moment is similar to the single magnitude 7 event. Thus a less-rare or "most perceptible" earthquake that is felt and causes damage on the greater number of occasions than the maximum credible most-rare possibility is preferable as a design earthquake for conventional buildings (Burton et al., 1984, 2004).

The CSER in Figure 2a for entire Java is dominated by the 1994 June 2 earthquake with magnitude 7.8 M_W (with epicentre at 10.48°S, 112.83°E). This magnitude is akin in size to the Kashmir 2005 October 8 earthquake which had magnitude 7.6 M_W; focal depths also appear to have been reported similarly as 18 and in the range 13-26 km respectively. On this model the magnitude of the 1994 earthquake is very close to the maximum credible for all Java in the study area. The situation in the near-vicinity of Yogyakarta and the Bantul earthquake epicentre is quite different. Figure 2b (which excludes the Bantul earthquake) indicates a near-vicinity M_3 of ~6.6 M_S with waiting time in the region of 11 years, while including the Bantul earthquake only raises M_3 to ~6.62 M_S. Thus in the case of the Yogyakarta region adjacent to Bantul, the occurrence of the 6.3 M_W Bantul earthquake has hardly affected the calculation of the maximum credible magnitude on this model, indeed although slightly less, the Bantul magnitude is similar to the local maxcred magnitude. However, when ground shaking is considered later, a significant influence on ground shaking seismic hazard is observed largely due to the unusual nature of this magnitude 6.3 event, viz, its shallowness in relation to most of the regional magnitude 6s.

It is also worthy of note that cumulative strain energy release depicted in Figure 2c has reached the upper enveloping line; at face value this might suggest that currently there is little strain energy to be released in the near-vicinity of the Bantul earthquake and a period of strain energy accumulation might be in preparation. However, it must be emphasised that this is on the analysis basis of an extremely limited duration earthquake catalogue and complacency is not in order.

This method usefully embraces earthquakes that have occurred but cannot be linked explicitly to a specific mapped fault and will of course include earthquakes that have occurred on faults that are known and active without being fault specific; clearly it does not take account of currently aseismic faults, known or unknown, and does not distribute strain energy or seismic moment release amongst selected faults of a regional fault ensemble. For example, the Central Java area has many faults that crisscross the area south of Mt Merapi and into the Wonosari basin to the east. Detailed evaluation of surficial fault activity and capability, which would be appropriate particularly for high consequence facilities, requires long term programmes whereas there are immediate needs to determine reasonable assessments and views on seismic hazard and corresponding mitigation measures. This is the first and non-probabilistic approach to establish an estimate of one important parameter of magnitude hazard – the maximum credible earthquake magnitude that is possible within a GIS scenario indicate worst conceivable consequences of an earthquake and assist mitigation planning.

Magnitude Hazard from "Extremes"

The second approach adopted is entirely probabilistic and is based on Gumbel's extreme value theory. Annual extreme values of magnitude are extracted from the study catalogue and Gumbel's third distribution fitted to this reduced dataset. This approach is consistent with the need to examine the larger earthquakes that tend to be the more damaging, and the statistical distribution itself is compatible with the physics of earthquakes in that earthquake magnitude is upper bounded:

$$GIII(m) = \exp\left[-\left(\frac{\omega - m}{\omega - u}\right)^k\right] \quad (1)$$

in which the asymptotic upper bound to magnitude is the parameter ω, u is the characteristic extreme value, k relates to curvature of the distribution and is often given as λ where $k = 1/\lambda$, and $GIII(m)$ is the probability that magnitude m is an extreme.

The details of the distribution and fitting it to seismicity data have been developed and reviewed elsewhere (e.g. Burton et al., 2004). In brief extreme values are extracted from an earthquake catalogue at predetermined time intervals (e.g. annually or biannually etc.), either directly as in maximum magnitude in each time interval or through appropriate relationships for peak ground acceleration (PGA). These are then ranked and the statistical distribution equation (1) fitted to these data so that probabilities of occurrence can be attached to magnitude ranges (or PGAs) for forecasting purposes, i.e. seismic hazard assessment.

Local variations in seismic hazard are resolved and mapped by dividing the area into a net of cells, to capture earthquakes, and a matrix of grid points. Each grid point is at the centre of a cell. Earthquakes within each cell are used to determine parameters of the Gumbel distribution fitted to the observed seismicity data. Hazard values at specific probabilities and return periods are then assigned to the cell-centre grid point for each cell analysed and these values are then mapped and contoured. Cells are designed to overlap to obtain detailed information throughout the study region.

In the present analysis strategy a 2° square cell is adopted moving through the catalogued seismicity by 0.5° intervals. Results for the parameter set $\{\omega, u, \lambda\}$ for each 2° cell are then used to calculate the arbitrary but consensually adopted statistic (e.g by the Global Seismic Hazard Assessment Program, GSHAP, 1999) of the 50-year earthquake with 90% probability of not being exceeded (p.n.b.e.). There is a one-in-ten chance that this magnitude will be exceeded in any 50-year period; this can be expressed equivalently as this magnitude has an average return period of 475 years. For example for the 2° square cell, centred at 8°S 110.5°E corresponding approximately to the region near Yogyakarta (note Yogyakarta is typically assigned the spot point coordinate 7°49′S 110° 22′E), the associated magnitude hazard can be expressed in terms of the magnitude (and PGA, see later) at a given return period or probability (Table 1a) or conversely, at return periods for a given magnitude (Table 1b).

Table 1. Magnitude hazard near Yogyakarta in terms of a) magnitude at fixed return period (and probability), and b) return period for fixed magnitude

a) Magnitude at fixed return period (and probability)			
	50-yr (90% p.n.b.e)	50-yr	100-yr
Magnitude M_s	6.9	6.7	6.8
b) Return period for fixed magnitude			
	5.5 M_s	6.0 M_s	6.5 M_s
Return Period (years)	3	7	28

Our results from this strategy for all Java are then contoured in Figure 3. The magnitude seismic hazard parameter of Table 1a column 2 is selected from all cells i.e. the earthquake magnitude that has one-in-ten chance of being exceeded in 50 years. This is magnitude seismic hazard for the solid volume contained below the two-dimensional surface of each cell, many of these recurring earthquakes are at considerable depth in the seismotectonic environment below the surface of Java, and not shallow like the Bantul earthquake. The Bantul earthquake was unusual and although a member of the set of earthquakes with magnitude greater than 6 M_W, it is in itself an unusual member. In terms of generation of the map in Figure 3 we hold a database of similar results for all cells for all Java, but this is too large to publish here.

Results for the parameter set $\{\omega,u,\lambda\}$, with standard deviations, for a cell analysis specifically chosen to be centred on the Bantul earthquake epicentre are $\{\omega,u,\lambda\}$ = (6.78 ± 1.02, 3.62 ± 0.52, 0.53 ± 0.39) excluding covariances.

Ensuing forecasts using these $\{\omega,u,\lambda\}$ to calculate the magnitude with an average return period of 50, 100 and 200 years have means respectively of 6.51, 6.59 and 6.65, and with 90% p.n.b.e. for 50, 100 and 200 years have means respectively of 6.66, 6.70 and 6.72.

GROUND SHAKING HAZARD (PEAK GROUND ACCELERATION)

The next objective in this study is to obtain a preliminary estimate of earthquake strong ground shaking seismic hazard in which the parameter of shaking is the earthquake engineering convention of peak ground acceleration (PGA). The strong motion attenuation law adopted is that of Patwardhan et al. (1978) as reported in Idriss (1978): this is a selection based on reasonable pertinence and relevance to the region given the lack of a satisfactory review of currently best practise on this important issue for this region, Java, and so Patwardhan et al. is used in the following form:

$$\ln(PGA) = \ln(A) + B\,M_S + E\,\ln[R + d\exp(f\,M_S)] \quad \text{......................................} (2)$$

where PGA is in cm s^{-2}, d = 0.864 and f = 0.463 (for stiff soil with A = 363 for the mean, B = 0.587 and E = -1.05). Note Eq(2) is in terms of M_S which is compatible with the earthquake catalogue created. The statistical model adopted to analyse computed values of PGA using Eq(2) is again extreme values but now is the Gumbel first asymptotic distribution of extreme values. Results obtained for the PGA with a one-in-ten chance of being

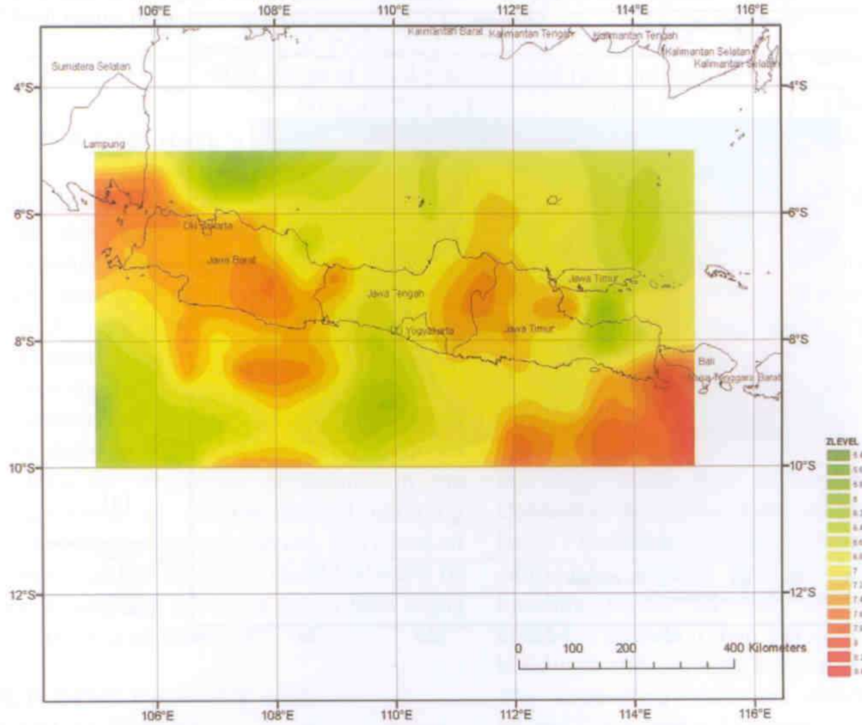

Figure 3. Magnitude hazard: contours of 50-year earthquake magnitude M_S with one-in ten chance of exceedance.

exceeded in any 50-year period are contoured in Figure 4. Figure 4a shows the results of this seismic hazard analysis on seismicity data 1973 through 2005 and Figure 4b on seismicity data 1973 through 2006/05/27 i.e. now including the Bantul earthquake.

The analysis strategy is similar to that described above for magnitude seismic hazard, although it is important to draw distinctions. Earthquake occurrence is a point process whereas the strong ground shaking that an earthquake produces propagates and spreads out from the focus and is thus a field process or field effect with strong ground shaking felt everywhere, at every point, out to the radius of perception of the earthquake.

Figure 4a indicates Yogyakarta is in a zone expecting circa 100-199 cm s^{-2} whereas Figure 4b now indicates circa 200-299 cm s^{-2} in the near-vicinity and even 300+ cm s^{-2}. The occurrence of the Bantul earthquake has simply extended the zone seen south offshore Yogyakarta in Figure 4a towards the northwest and to Yogyakarta in Figure 4b. Extracting results, as illustrative examples, from two points of analysis near Yogyakarta (7.5°S 110.5°E and due south at 8°S 110.5°E) provides ground shaking ranges for PGA at different hazard or probability levels in Table 2. These two illustrative points of analysis in Table 2 fall inside the new red spot in the map of Figure 4b and just to the north of Yogyakarta Province.

Again, similarly to the map in Figure 3, in terms of the generation of the map in Figure 4b we have a database of similar results for all cells for all Java (more extensive in variety of PGA seismic hazard parameters than indicated in Table 2, for

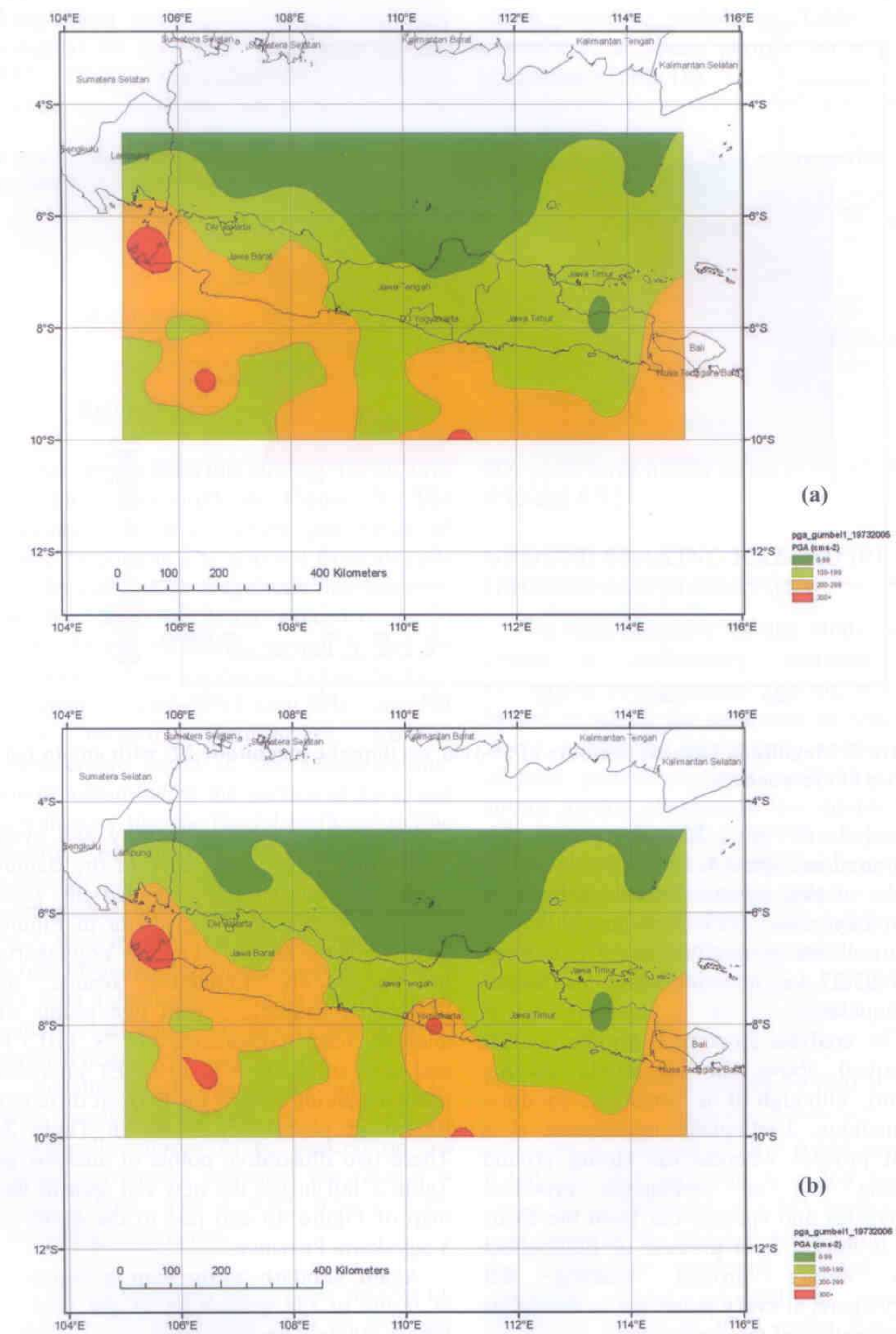

Figure 4. Ground shaking hazard: contours of 50-year PGA with one-in-ten chance of exceedance, a) earthquake catalogue data 1973-2005 and b) 1973-2006/05/26 including the Bantul earthquake.

Table 2. Peak ground acceleration hazard ranges spanning two points of assessment: just to the north of Yogyakarta Province (lower value in range) and within Yogyakarta (higher value in range) in terms of fixed return period and probability

	PGA range at fixed return period (and probability)		
	50-yr (90% p.n.b.e)	50-yr	100-yr
PGA range (cm s^{-2})	191-349	122-228	144-266

example for each cell point analysed there exist the distribution parameters with covariance matrix and uncertainties on the PGA forecasts etc.), again too large to publish.

Further work should be done on improving the earthquake catalogue and on generation of strong motion attenuation laws deriving from strong motion observed in Java for maximum pertinence in the development of seismic hazard mapping and ensuing mitigation advice. Revisions of seismic hazard mapping should always be seen as ongoing guidance rather than being conclusive and definitive.

BUILDING DAMAGE AND DISPLACEMENT

Observations of Building Damage in Kashmir and Java

The maximum intensity levels observed in 2005 Kashmir reached to about intensity X MSK (perhaps assisted by some examples of local amplification on ridge-like structures) and in 2006 Bantul to about intensity IX MSK (assisted in some cases by localised liquefaction and soft soil effects). PGA values of order 200 and 300 cm s^{-2} dominate the near-vicinity or zone of Yogyakarta in Figure 4b and such values have historically been considered commensurate with intensities around VIII or IX MSK. Figure 5 provides some examples of building damage modes observed in 2005 Kashmir and one example in 2006 Bantul; these photographs are examples amongst other observations indicative of such high level macroseismic impacts on vulnerable buildings in both earthquakes.

The detail in Figures 5a-d of damage or collapse mode is both fascinating and informative. The locality of these four photographs is a few km north of Muzaffarabad (capital of North West Frontier Province, NWFP, Kashmir) and at ~18 km from the epicentre. The eastern areas of NWFP showed some of the most severe damage, for example in Balakot and Muzaffarabad (EEFIT, 2006). In the background of Figure 5b can also be seen the large white area of freshly exposed Dolomitic limestone that resulted from a large landslide at the time of the earthquake. Figures 5c-d are of the same building, Figure 5d being slightly further along the right of it than in Figure 5c. These buildings and damage impacts are typical. The supporting walls are either concrete block (Figures 5a,c-d) or concrete block in-fill walls with reinforced concrete (RC) columns. In all cases the wall/column structure supports a heavy roof. In cases Figure 5a,c a large heavy water tank can also be seen on the respective roof remains. In all three cases these buildings are effectively inverted pendula and have behaved as such during the earthquake with catastrophic consequences.

Note the walls supporting the water tank in Figure 5a. The wall facing the camera shows classic "X" shaped shear crack development, and the base of this wall has moved with the foundation and the earth to the left. The causative fault is to the left and behind this building (by of order 1 km). In Figure 5b the fault is near the newly exposed white area of limestone landslide; the RC columns lean out and right from the photograph as the foundation moved inwards and leftwards towards the fault. The RC columns of the building in Figures 5c-d lean into the photograph, inwards and leftwards, in response to the foundations and earth moving in a direction out and right from the photograph and towards the fault. Figure 5d is particularly dramatic and diagnostic. When the horizontal ground displacement pulse arrived at this building the foundations moved towards the fault, given the inertial properties of the heavy roof the roof remained where it was (for a short while), the RC columns thus toppled and leaned away from the vertical inwards to the photograph – until the roof was no longer supported by the RC columns and simply fell off the columns under gravity to the ground – complete pancake collapse mode. The Kashmir earthquake had thrust mechanism which is entirely consistent with the building foundations in Figures 5a-d displacing rapidly horizontally *towards* the fault.

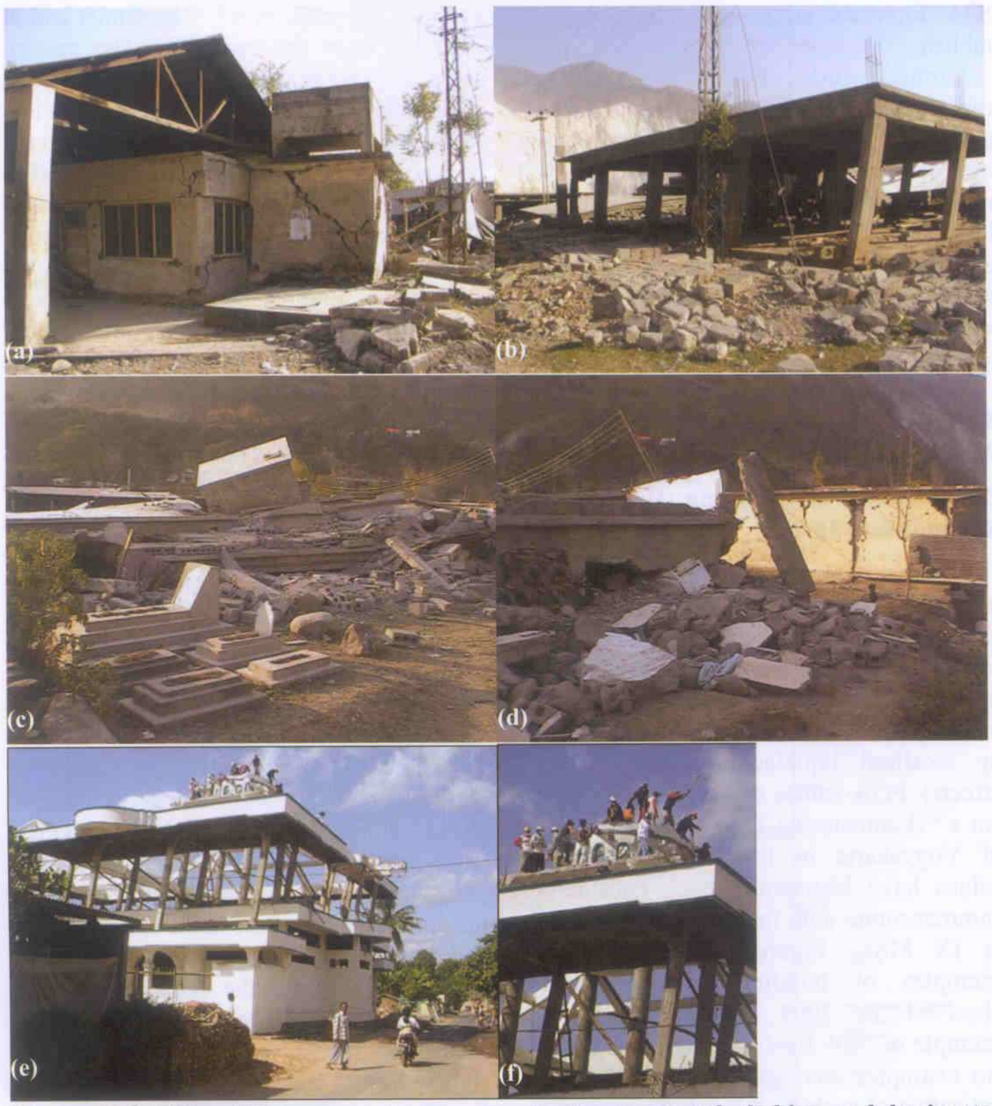

Figure 5. Building failure mode in response to strong ground shaking and horizontal displacement: a-d) buildings near Muzafarrabad, Kashmir earthquake, e-f) Bantul earthquake. Note c-d are the same building. See text for description. (Photos a-d: Paul Burton. Photos e-f: BBC News).

Horizontal Displacement Field

The displacement field of the Kashmir earthquake has been investigated using satellite observation (Wright and Pathier, personal communications; Pathier et al., 2006) and a modified version of their horizontal displacement observations and analysis are shown in Figure 6. These methods using satellite observation techniques appear not to have been attempted to assess deformation in the Yogyakarta Basin, probably because the smaller magnitude Bantul earthquake caused considerably lesser distributed deformations confined relatively close to the Opak fault. Even though the Bantul earthquake epicentre was 10 km east of the Opak fault in the Wonosari basin the causative fault is not unequivocally determined.

The abrupt change from red to white in Figure 6 indicates the NW-SE strike of the Muzafarrabad-Tanda fault. The small arrows in Figure 6 are proportional to horizontal displacement. At Muzafarrabad (labelled f in Figure 6a, zoomed from the regional field of Figure 6b) the horizontal displacement is approximately towards the NNE. Tentatively revisiting the building in Figure 5b it should be noted that the white landslide scar is east of the building. The alignment of the leaning RC columns, best seen in the foreground, is therefore leaning towards the ~SSW consistent with ~NNE horizontal displacement of the foundations accompanying the horizontal displacements of the fault. Earthquake engineers, urban and rural builders, still have much to implement from an understanding of old fashioned, massy, displacement seismology. Designers, planners, owners and government officials need to understand many facets of the seismic hazards that they face, including the interaction between strong ground shaking, usually expressed through simple PGA values, and vulnerability and hence risk associated with local building stocks and building practices. In addition to this they also need to understand building behaviour near to capable faults, where ground displacements may be large and have significant influence on a catastrophic mode of building failure.

The behaviour of columns supporting heavy roofs during the Bantul earthquake is worthy of comparison. The example in Figures 5e-f shows unsupported columns leaning presumably in response to earthquake horizontal displacement. Roof collapse stage was not reached in this example. Whereas the Kashmir earthquake had thrust mechanism the Bantul earthquake was strike-slip but without clear surface rupture and equivalent fault defining features. Detailed observations of horizontal displacement induced building impacts, as well as providing future mitigation data for building construction, may also reveal spatial patterns of damage indicative of local capable fault dynamics. The directional properties of the step or pulse of displacement caused by the rupturing fault might be mapped at the surface through this means, although fault rupture itself can not be adequately mapped in the field. From a practical stand point, buildings with out-of-plane walls (in relation to the direction of horizontal displacement) that are weak, extensive, uncontained and unsupported are likely to be pushed over, just as columns supporting relatively heavy roofs are also likely to be pushed out of the perpendicular and precipitate roof collapse.

CONCLUSIONS

CSER analyses indicate a maximum credible magnitude approximately 6.6 M_S within a 2° area centred on the Bantul epicentre. The Bantul earthquake was at 6.3 M_W close in magnitude to this worst conceivable occurrence. CSER also suggests this zone near Yogyakarta may now enter a period of strain accumulation rather than release. This does not provide reason for complacency on two grounds: 1) the earthquake history analysed only extends back to 1973 (early instrumental, historical and even palaeoseismic evidence

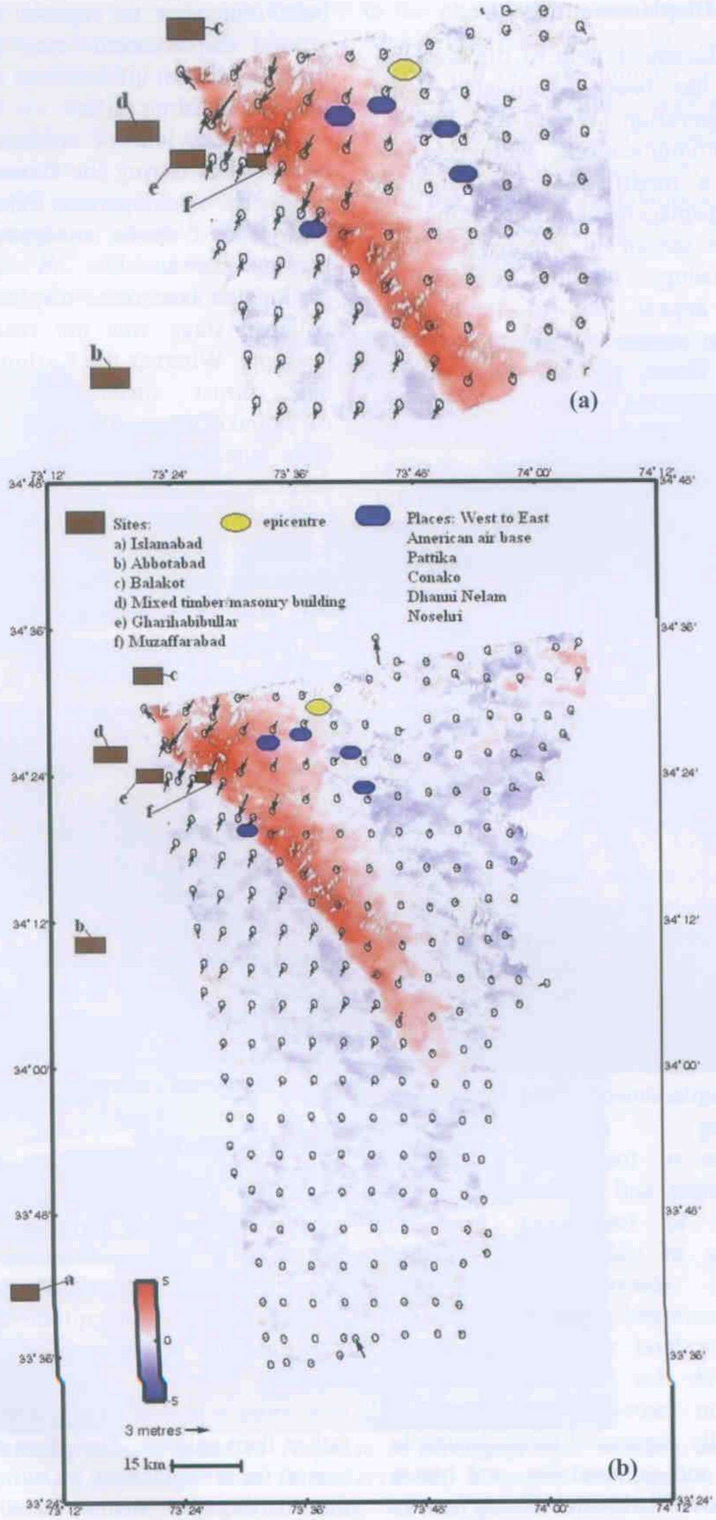

Figure 6. Horizontal displacement: Kashmir earthquake (adapted T. Wright and E. Pathier, personal communications; Pathier et al., 2006).

should be sought to extend this) and 2) PGA hazard analysis indicates near-vicinity Yogyakarta is in a zone that has 50-year expectation (one-in-ten chance of exceedance) of 200-300+ cm s^{-2}. Ordinary building stock should be built to withstand such levels of vibration without catastrophic collapse. Building mode failure in relation to horizontal displacement caused by the Bantul earthquake in the zone near to the Opak fault should also be investigated because near-fault displacements close to the capable causative fault may be controlling catastrophic collapse failures – possible remedies might emerge through building codes that improve column stability via-a-via roof weight, and which consider the area, containment and support of large walls. A full study of seismic hazard, vulnerability, risk assessment and ensuing recommendations for population welfare that would take account of in situ observations would be highly desirable and is recommended.

ACKNOWLEDGEMENTS

The Engineering and Physical Sciences Research Council funded work in Pakistan. An Earthquake Engineering Field Investigation Team (Peiris, Mahmood, Rossetto, Burton), Institution of Structural Engineers, London carried out field work with members of Peshawar University. Tim Wright and Erwan Pathier provided valuable material. Robert Anderson's comments helped us to improve the paper. The credit for two photographs used herein goes to the BBC whom we thank.

REFERENCES

Burton, P.W., R.W. McGonigle, K.C. Makropoulos, and S.B. Ucer, 1984, Seismic Risk in Turkey, the Aegean, and the Eastern Mediterranean: the Occurrence of Large Magnitude Earthquakes, Geophys. J. R. astr. Soc., **78**, p. 475-506.

Burton, P.W., C. Qin, G-A. Tselentis, and E. Sokos, 2004, Extreme Earthquake and Earthquake Perceptibility Study in Greece and Its Surrounding Area, Natural Hazards, **32**, p. 277-312.

EEFIT, 2006, Peiris, N., T. Rossetto, P. Burton, and S. Mahmood, EEFIT Mission: October 8, 2005 Kashmir Earthquake, Preliminary Report, Earthquake Engineering Field Investigation Team, 31 pages, http://www.istructe.org.uk/eefit/files/EEFIT%20Mission%20Pakistan%20-%20prelim%20report.pdf, www.eefit.org.uk.

GSHAP, 1999, D. Giardini (ed.), The Global Seismic Hazard Assessment Program (GSHAP) 1992-1999, Summary Volume, Annali di Geofisica, **42**, 6, p. 957-1230.

Makropoulos, K.C. and P.W. Burton, 1984, Seismic Risk of Circum-Pacific Earthquakes. I: Strain Energy Release, Pure appl. Geophys., **121**, p. 147-167.

Pathier, E., E.J. Fielding, T.J. Wright, R. Walker, B.E. Parsons, and S. Hensley, 2006, Displacement Field and Slip Distribution of the 2005 Kashmir Earthquake From SAAR imagery, Geophys. Res. Letters, **33**, L20310, doi:10.1029/2006GL027193, p. 5.

Patwardhan, A., K. Sadigh, I.M. Idriss, and R. Youngs, 1978, Reported in I.M. Idriss, 1978, Characteristics of Earthquake Ground Motions, Proceedings of the ASCE Geotechnical Engineering Division Speciality Conference: Earthquake Engineering and Soil Dynamics, vol. III (June), p. 1151-1265.

Rezapour, M., and R.G. Pearce, 1998, Bias in Surface-Wave Magnitude M_S due to Inadequate Distance Corrections, Bull. Seis. Soc. Am., **88**, p. 43-61.

The Yogyakarta Earthquake of May 27, 2006

Edited by:
Dwikorita Karnawati
Subagyo Pranumijoyo
Robert Anderson
Salahuddin Husein

Star
PUBLISHING COMPANY, INC.

PUBLISHING COMPANY, INC.

Star Publishing Company, Inc.
Belmont, CA 94002

www.starpublishing.com

Library of Congress Cataloging-in-Publication Data

The Yogyakarta earthquake of May 27, 2006 / edited by Dwikorita Karnawati ... [et al.]. -- 1st ed.
p. cm.
Includes bibliographical references.
ISBN 978-8898633074
1. Yogyakarta Earthquake, Indonesia, 2006. 2. Earthquakes--Indonesia--Yogyakarta. I. Karnawati, Dwikorita.

QE536.2.I5Y94 2008
363.34'950959827--dc22
2007040289

ISBN: 978-0-89863-304-7

Printed in Korea

12 11 10 09 08 07 · 10 9 8 7 6 5 4 3 2 1